Inorganic Chemistry

Article

pubs.acs.org/IC

Stabilization of Tetravalent 4f (Ce), 5d (Hf), or 5f (Th, U) Clusters by the $[\alpha\text{-}SiW_9O_{34}]^{10-}$ Polyoxometalate

Sylvain Duval,*[,†] Sébastien Béghin,[†] Clément Falaise,[†] Xavier Trivelli,[‡] Pierre Rabu,[§,∇] and Thierry Loiseau[†]

[†]Unité de Catalyse et Chimie du Solide (UCCS)−UMR CNRS 8181, Université de Lille Nord de France, USTL-ENSCL, Bat C7, BP 90108, 59652 Villeneuve d'Ascq, France

[‡]Unité de Glycobiologie Structurale et Fonctionnelle (UGSF)−UMR CNRS 8576, Université de Lille Nord de France, Bat C9, BP 90108, 59652 Villeneuve d'Ascq, France

[§]Institut de Physique et Chimie des Matériaux de Strasbourg, UMR 7504 CNRS-University of Strasbourg, 67034 Strasbourg cedex 2, France

[∇]International Center for Frontier Research in Chemistry (icFRC), 8, Allée Gaspard Monge, F-67000, Strasbourg, France

Supporting Information

ABSTRACT: The reaction of $Na_{10}[\alpha\text{-}SiW_9O_{34}]$ with tetravalent metallic cations such as 4f ($(NH_4)_2Ce(NO_3)_6$), 5d ($HfCl_4$), or 5f (UCl_4 and $Th(NO_3)_4$) in a pH 4.7 sodium acetate buffer solution leads to the formation of four sandwich-type polyoxometalates $[Ce_4(\mu^3\text{-}O)_2(SiW_9O_{34})_2(CH_3COO)_2]^{10-}$ (**1**), $[U_4(\mu^3\text{-}O)_2(SiW_9O_{34})_2(CH_3COO)_2]^{10-}$ (**2**), $[Th_3(\mu^3\text{-}O)(\mu^2\text{-}OH)_3(SiW_9O_{34})_2]^{13-}$ (**3**), and $[Hf_3(\mu^2\text{-}OH)_3(SiW_9O_{34})_2]^{11-}$ (**4**). All four compounds consist of a polynuclear cluster fragment stabilized by two $[\alpha\text{-}SiW_9O_{34}]^{10-}$ polyanions. Compounds **1** and **2** are isostructural with a tetranuclear core (Ce_4, U_4), while compound **3** presents a trinuclear Th_3 core bearing a μ^3-O-centered bridge. It is an unprecedented configuration in the case of the thorium(IV) cluster. Compound **4** also possesses a trinuclear Hf_3 core but with the absence of the μ^3-O bridge. The molecules have been characterized by single-crystal X-ray diffraction, ^{183}W and ^{29}Si nuclear magnetic resonance (NMR) spectroscopy, infrared (IR) spectroscopy, thermogravimetric analysis (TGA), and scanning electron microscopy/energy-dispersive X-ray (SEM/EDX) analysis.

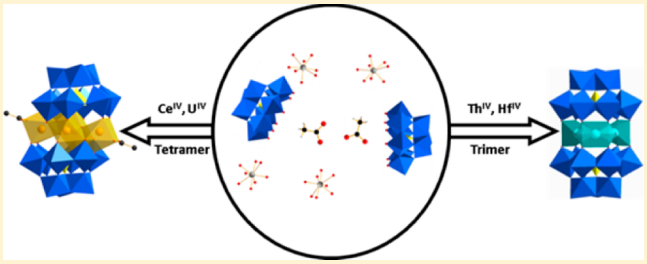

1. INTRODUCTION

Heteropolyoxometalates (POMs) are discrete molecular assemblies based on the condensation of transition metals. They are known for their large composition and structural diversity, making them attractive for their properties in catalysis, magnetism, materials science, or luminescence.[1−8] POMs are usually constructed from polycondensation processes, in aqueous acidic solution, of metal-oxo species. Incorporation of various templating agents (using tetrahedral XO_4 units, where X = P^V, Si^{IV}, Ge^{IV}, etc., or trigonal XO_3 units, where X = As^{III}, Sb^{III}, Bi^{III}, etc.) or heterometals increase the structural diversity of this family of molecules and helps to modulate the properties of the related materials. This also can be obtained via controlled hydrolysis with vacant polyoxometalates species. For instance, trivacant Keggin polyoxometalates are particularly known in POM chemistry to act as a polydentate ligand, thus allowing the coordination of different metallic species. Most examples found in the literature include sandwich-like compounds with incorporation of polymetallic 3d and 4d transition-metal−oxo clusters (for example, see the nonexhaustive series of compounds containing Fe, Co, Zr, Mo, etc.).[9−13] Over the years, the heterometallic core in these compounds have a tendency to grow in nuclearity. From this point of view, we are interested in the use of such inorganic moieties to coordinate clusters of tetravalent 4f (cerium), 5d (hafnium), and 5f (uranium, thorium) cations. To our knowledge, only few examples of polyoxometalates coordinated to tetravalent 4f, 5d, or 5f metallic cations have been described in the literature. They are built from the association of vacant Keggin- or Dawson-type polyoxotungstates associated with tetravalent metallic cations (zirconium, hafnium, cerium, uranium, or thorium), sometimes mixed with 3d metals, giving rise to 1:2 sandwich-type compounds, such as $[M^{IV}(XW_{11}O_{39})_2]^{12-}$, $[M^{IV}(XW_{17}O_{61})_2]^{16-}$, or more-complex sandwiched systems $[\{M^{IV}(H_2O)\}_2(\mu\text{-}OH)_2(\gamma\text{-}SiW_{10}O_{36})_2]^{10-}$ and $[\{M^{IV}(H_2O)\}_4(\mu^4\text{-}O)(\mu\text{-}OH)_6(\gamma\text{-}SiW_{10}O_{36})_2]^{8-}$ (with M = Zr, Hf, Ce, U, Th and X = P, Si, Ge).[14−28] Some more-complex molecules with three or six condensed metallic zirconium and hafnium cations were also obtained by various groups.[29,30] Recently, some of these complexes containing tetravalent uranium were characterized by small-angle X-ray scattering.[31]

Received: April 8, 2015

DOI: 10.1021/acs.inorgchem.5b00786
Inorg. Chem. XXXX, XXX, XXX−XXX

Table 1. Crystal Data and Structure Refinement for Compounds 1−4

	1	2	3	4
formula	$C_4H_6Ce_4Cs_{1.5}Na_{8.5}O_{97.5}Si_2W_{18}$	$C_4H_6U_4Cs_3Na_7O_{97.7}Si_2W_{18}$	$Na_{12}RbO_{98}Si_2Th_3W_{18}$	$Na_3Rb_{8.5}O_{95.25}Cl_{0.5}Si_2Hf_3W_{18}$
formula weight	5934.83	6494.55	5990.95	6238.14
temperature	100 K	100 K	100 K	100 K
crystal color	yellow	dark brown	colorless	colorless
crystal size	0.20 mm × 0.15 mm × 0.15 mm	0.45 mm × 0.15 mm × 0.10 mm	0.30 mm × 0.15 mm × 0.15 mm	0.40 mm × 0.40 mm × 0.20 mm
crystal system	monoclinic	monoclinic	trigonal	triclinic
space group	$C2/c$	$C2/c$	$P63/m$	$P\bar{1}$
a	25.7962(8) Å	25.8519(12) Å	12.1735(3) Å	12.6921(5) Å
b	19.0538(5) Å	19.0881(9) Å	12.1735(3) Å	16.9827(7) Å
c	18.0991(5) Å	18.1113(9) Å	33.1941(8) Å	21.3707(10) Å
α	90°	90°	90°	94.684(2)°
β	100.5227(15)°	100.472(3)°	90°	97.557(2)°
γ	90°	90°	120°	101.571(2)°
volume	8746.4(4) Å^3	8788.4(7) Å^3	4260.13(18) Å^3	4445.8(3) Å^3
Z	4	4	2	2
density, $\rho_{calculated}$	4.6153 g cm^{-3}	4.9481 g cm^{-3}	4.6701 g cm^{-3}	4.66 g cm^{-3}
μ	26.411 mm^{-1}	32.206 mm^{-1}	30.191 mm^{-1}	31.466 mm^{-1}
θ range	1.34°−26.58°	1.33°−26.57°	1.23°−33.17°	1.48°−36.40°
limiting indices	$-32 \le h \le 32$	$-31 \le h \le 32$	$-18 \le h \le 18$	$-15 \le h \le 15$
	$-23 \le k \le 23$	$-23 \le k \le 23$	$-18 \le k \le 18$	$-21 \le k \le 21$
	$-22 \le l \le 22$	$-19 \le l \le 22$	$-51 \le l \le 25$	$-26 \le l \le 26$
collected reflections	60648	45044	46721	110396
unique reflections	9055	9060	5525	18167
	[R(int) = 0.0376]	[R(int) = 0.0693]	[R(int) = 0.0579]	[R(int) = 0.0506]
parameters	614	370	218	758
goodness-of-fit on F^2	1.093	1.034	1.291	1.081
final R indices [$I > 2\sigma(I)$]	R_1 = 0.0271	R_1 = 0.0512	R_1 = 0.0331	R_1 = 0.0381
	wR_2 = 0.0611	wR_2 = 0.1311	wR_2 = 0.0694	wR_2 = 0.904
R indices (all data)	R_1 = 0.0318	R_1 = 0.0697	R_1 = 0.0359	R_1 = 0.0416
	wR_2 = 0.633	wR_2 = 0.1447	wR_2 = 0.0702	wR_2 = 0.922
largest diff. peak and hole	1.97 and −1.77 e Å^{-3}	4.19 and −6.19 e Å^{-3}	2.25 and −2.53 e Å^{-3}	4.29 and −4.85 e Å^{-3}

Generally, these types of tetravalent clusters are not easily stabilized or crystallized from solution. They generally require the presence of several organic acids or amino acids to prevent the infinite condensation process of the metallic cations and stop at a nanoparticle size in discrete coordination compounds. Some nice recent examples included an octanuclear thorium cluster organized in a boat shape and stabilized by coordination of several selenite oxides,[32] polynuclear cerium clusters up to 22 metal centers,[33] and an U_{38} nano poly oxo cluster composed of tetravalent uranium and containing distorted UO_2 fluorite core, which is stabilized by THF solvent molecules and benzoate ligands.[34] The recent reports of Knope and Soderholm[35] and Nyman and Burns[36] gave a good survey of the poly oxo clusters occurrence for actinides.

Herein, we report on the synthesis, characterization, and structural description of four new sandwich-type polyoxometalates containing 4f, 5d, and 5f polyoxometallic clusters, $Cs_2Na_8[Ce_4(\mu^3\text{-}O)_2(SiW_9O_{34})_2(CH_3COO)_2]\cdot 40H_2O$ (**1**), $Cs_3Na_7[U_4(\mu^3\text{-}O)_2(SiW_9O_{34})_2(CH_3COO)_2]\cdot 24H_2O$ (**2**), $Na_{12}Rb[Th_3(\mu^3\text{-}O)(\mu^2\text{-}OH)_3(SiW_9O_{34})_2]$ (**3**), and $Rb_{8.5}Na_3[Hf_3(\mu^2\text{-}OH)_3(SiW_9O_{34})_2]Cl_{0.5}\cdot 24H_2O$ (**4**). These molecules are built from the association of tetravalent cerium, hafnium, uranium, and thorium cations with the trivacant $[SiW_9O_{34}]^{10-}$ polyoxometalate.

2. EXPERIMENTAL SECTION

Synthesis. *Caution! Uranyl chloride (UCl_4) and thorium nitrate ($Th(NO_3)_4\cdot 4H_2O$) are radioactive and chemically toxic reactants, so precautions with suitable care and protection for handling such substances have been followed.*

The compounds have been synthesized by using the following chemical reactants: ammonium cerium nitrate ($(NH_4)_2Ce^{IV}(NO_3)_6$, Acros Organics, 99%), uranyl chloride (UCl_4, obtained from the protocol using the reaction of hexachloropropene with uranium oxide), thorium nitrate ($Th(NO_3)_4\cdot 4H_2O$, Prolabo, 99.99%), Cs-(NO_3) (Aldrich, 99%), CsCl, Rb(NO_3) (Alfa Aesar, 99.8%), RbCl (Acros Organics, 99.8%), and acetate buffer (solution made by using glacial acetic acid (Carlo Erba reagent, 99.9%) and sodium acetate (Merck, 99%)). The starting chemical reactants (except UCl_4) are commercially available and have been used without any further purification. $Na_{10}[SiW_9O_{34}]\cdot 12H_2O$ was synthesized according to a literature procedure.[37]

Compound 1. $(NH_4)_2Ce^{IV}(NO_3)_6$ (328 mg, 0.60 mmol) was dissolved in 5 mL of a 1 M sodium acetate buffer (pH 4.7). $Na_{10}[SiW_9O_{34}]\cdot 12H_2O$ solid (500 mg, 0.20 mmol) was added to the cerium solution. The resulting mixture was heated at 50 °C for 30 min until the yellowish solid dissolved. Cs(NO_3) (13 mg, 0.067 mmol) was added to the solution, which was heated for an additional 15 min at 50 °C. The solution was cooled to room temperature and left to crystallize by slow evaporation. After 1 day, yellow crystals suitable for X-ray diffraction (XRD) analyses started to appear. After 1 week, the crystals were filtered off, washed with a small amount of water, and dried at room temperature (mass (m) = 112 mg, yield = 18%).

IR (cm^{-1}): 996(w), 956(m), 872(s), 852(m), 793(s), 757(s), 717(s), 673(s), 643(s), 516(s).

Compound 2. $Na_{10}[SiW_9O_{34}]\cdot 12H_2O$ (250 mg, 0.10 mmol) was dissolved in 10 mL of 1 M acetate buffer (pH 4.7). The solution was added to solid UCl_4 (108 mg, 0.30 mmol). The brown solution was stirred for 10 min and CsCl (24 mg, 0.14 mmol) was added to the

DOI: 10.1021/acs.inorgchem.5b00786
Inorg. Chem. XXXX, XXX, XXX−XXX

solution. After stirring for an additional 10 min, the solution was left to crystallize at room temperature. After one night, brown crystals suitable for XRD analyses started to appear. The crystals were quickly collected (m = 45 mg, yield = 14%) before crystallization of $Na[U^{VI}O_2(OAc)_3]$ (OAc = acetate) as yellow crystals,[38] indicating the oxidation of the uranium.

IR (cm^{-1}): 996(w), 952(m), 875(s), 851(m), 789(s), 759(s), 724(s), 674(s), 647(s), 514(s).

Compound **3**. $Na_{10}[SiW_9O_{34}]\cdot 12H_2O$ (310 mg, 0.124 mmol) was dissolved in 3 mL of 1 M acetate buffer (pH 4.7). The solution was added to solid $Th(NO_3)\cdot 4H_2O$ (210 mg, 0.40 mmol). The colorless solution was stirred for 10 min and $Rb(NO_3)$ (14 mg, 0.095 mmol) was added to the solution. After stirring another 10 min, the solution was left to crystallize at room temperature. After 3 weeks, a mixture of a white microcrystalline powder and crystals suitable for XRD analyses was obtained.

IR (cm^{-1}): polyanion part: 983(w), 936(m), 863(m), 808(m), 769(m). Thorium acetate part: 1056(w), 1047(w), 1026(m), 956(m), 674(s), 639(s), 609(m), 498(s), 474(m).

Compound **4**. $HfCl_4$ (32 mg, 0.10 mmol) was dissolved in 7 mL of a 0.5 M acetate buffer (pH 4.7). $Na_{10}[SiW_9O_{34}]\cdot 12H_2O$ (250 mg, 0.10 mmol) was added to the metal solution, followed by the addition of 20 drops of 1 M RbCl solution until precipitation occurred. The solution then was heated to 60 °C for 15 min and cooled to room temperature and allowed to crystallize. After 2 days, suitable colorless crystals for XRD studies were obtained. The solution was left alone for 14 days and the crystals were collected (m = 90 mg, yield = 42.5%).

IR (cm^{-1}): polyanion part: 1014(w), 994(w), 938(m), 883(m), 750(s), 666(s), 527(s), 464(s).

Single-Crystal X-ray Diffraction. Crystals of **1**−**4** were selected under observation using a polarizing optical microscope and glued on a glass fiber or a mitegen loop for single-crystal XRD experiments. Because of the instability of the crystalline network, which is due to the loss of crystallization water, all measurements were performed at 100 K under a nitrogen flow. X-ray intensity data were collected on a Bruker Model X8-APEX2 CCD area-detector diffractometer using Mo Kα radiation (λ = 0.71073 Å) with an optical fiber as the collimator. Several sets of narrow data frames (10 s per frame) were collected at different values of θ for two initial values of ϕ and ω, respectively, using 0.3° increments of ϕ or ω. Data reduction was accomplished using SAINT V7.53a.[39] The substantial redundancy in data allowed a semiempirical absorption correction (SADABS V2.10)[40] to be applied, on the basis of multiple measurements of equivalent reflections. The structure was solved by direct methods, developed by successive difference Fourier syntheses, and refined by full-matrix least-squares on all F^2 data using the SHELX program suite.[41] Hydrogen atoms of the acetates ligands for compounds **1** and **2** were included in calculated positions and allowed to ride on their parent atoms. The final refinements include anisotropic thermal parameters of all non-hydrogen atoms, except the oxygen atoms of the water molecules and the atoms being NPD if refined anisotropically. The crystal data are given in Table 1. Supporting Information is available in CIF format.

NMR Spectroscopy. The ^{29}Si NMR and ^{183}W NMR measurements were carried out on 5 mm tubes. The crystals of compounds **1** and **4** were dissolved in a 90:10 H_2O/D_2O mixture (0.75 mL) to get a concentration of ∼25 mM. The spectra were recorded on a Bruker 400 MHz spectrometer. Chemical shift were referenced to the ^{183}W resonance of an external 2 M Na_2WO_4 solution in alkaline D_2O and ^{29}Si chemical shifts were referenced to TMS. The pH of the solutions is ∼5.2 for compound **1** and ∼5.4 for compound **4**.

Powder Diffraction. Microcrystalline powder patterns were recorded on a Bruker D8 Avance diffractometer (Cu Kα radiation) equipped with a lynx eye fast detector. Each pattern was recorded in the 2θ range of 5°−50° with a 0.5 s/step scan.

SEM/EDX Analysis. Photographs of the crystals were performed on a Hitachi Model S3400N system equipped with a tungsten filament. EDX measurements were performed on compounds **2** and **3** to estimate the Na/Cs and Na/Rb ratios, with respect to the rest of the molecular composition, and can be found in the Supporting Information (Figure S7).

Thermogravimetric Analysis. The thermogravimetric experiments have been carried out on a thermoanalyzer (SETARAM, Model TGA 92) under an air atmosphere with a heating rate of 1 °C min^{-1} from room temperature up to 600 °C for **1** and 800 °C for **2** and **4**. Compound **3** was not pure, so no TGA was performed on it.

Infrared Spectroscopy. Infrared spectra of compounds **1**−**4** were measured on Perkin−Elmer Spectrum Two spectrometer, between 4000 cm^{-1} and 400 cm^{-1}, that was equipped with a diamond attenuated total reflectance (ATR) accessory.

Magnetic Measurements. The magnetic properties of compound **2** have been investigated by using a Quantum Design Squid vibrating sample magnetometer (VSM). The temperature and field variation of the moment was measured on powder samples immobilized in a gelatin capsule. The magnetic susceptibility was measured under a field of 5000 Oe between 1.8 K and 300 K. The magnetization versus field variation was recorded between −70 000 Oe and +70 000 Oe. The measured magnetic moment was corrected for sample size effect, sample diamagnetism (based on Pascal's constant corrections[42,43]), and diamagnetism of the sample holder.

3. RESULTS

Synthesis. The four compounds have been synthesized in an acetate buffer solution at pH 4.7. SEM images of the crystals obtained after crystallization are presented in Figure S1 in the Supporting Information. The use of buffered solvent ensures that the solution will remain at a stable pH during the synthesis and crystallization processes. The pH of the solutions of the synthesis during the crystallization of the four compounds remains up to 4.2 with the cationic stoichiometry used in the synthetic procedure. Furthermore, as already seen in the literature,[44] the acetate ligands may be helpful regarding the control of the polycondensation processes of tetravalent species by playing the role of a ligand giving support to the coordination of the cluster. The tetravalent uranium cation is known to be unstable and, when subjected to air and water oxidation, form the uranyl $\{UO_2\}^{2+}$ species.[45] It is interesting to note that no precautions have been made regarding these oxidizing factors to obtain compound **2**. The stabilization of the 4+ oxidation state of uranium in this molecule can be explained using several parameters. The first one is the high charge density of the uranium atoms, causing a preferential electrostatic interaction with the oxygen atoms of the polyanion in the relatively acidic medium (buffer solution at pH ∼4.7). The second parameter is of geometric consideration. The U^{4+} atoms are located in the center of an "Archimedean" antiprism. The last factor is the unique electron transfer phenomenon occurring between the U^{4+} cations and the W^{6+} centers of the polyanion through the U−O−W bond observed in the sandwich complex $[U(P_2W_{17}O_{61})]^{16-}$.[46] This type of geometrical environment, which is present in the compounds $U(SO_4)_2\cdot 4H_2O$, $U(CH_3COO)_4$ and $U(C_2O_4)\cdot 6H_2O$, has been also shown to strongly stabilize the U^{4+} cation,[47−49] thus preventing the crystallized reduced form to be oxidized for several days even if the solid is left in the mother liquor.

Structure Description. The structures of compounds **1**−**4** consist of a sandwich-type polyoxometalate (Figure 1). In these molecules, the central heterometallic core corresponding to a tetranuclear group $\{M_4(\mu^3\text{-}O)_2\}$ (M = Ce, U) for **1** and **2**, respectively, and a trinuclear group $\{Th_3(\mu^3\text{-}O)(\mu^2\text{-}OH)_3\}$ for **3** or $\{Hf_3(\mu^2\text{-}OH)_3\}$ for **4**, are coordinated by the oxygen atoms of the vacancies of two $[SiW_9O_{34}]^{10-}$ subunits (Figure 1).

Compounds **1** and **2** are isostructural and each Ce^{4+} or U^{4+} center has a coordination number of eight with an

DOI: 10.1021/acs.inorgchem.5b00786
Inorg. Chem. XXXX, XXX, XXX−XXX

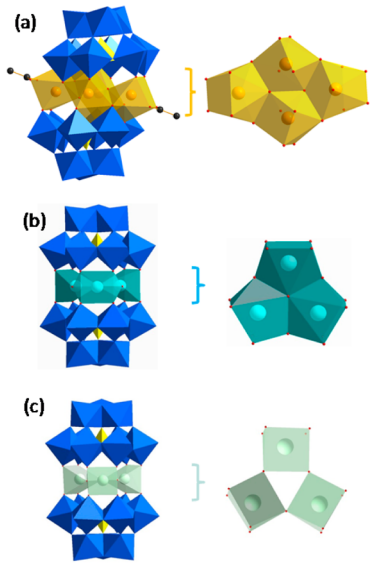

Figure 1. Polyhedral representations of the anionic part of (a) compounds **1** and **2**, (b) compound **3**, and (c) compound **4**. Side view on the left and top view of the central metallic cluster on the right.

"Archimedean" square antiprism geometry. Their tetravalent oxidation state was confirmed by BVS calculation (Table S2 in the Supporting Information).[50,51] Both systems crystallized in the monoclinic space group $C2/c$. The asymmetric unit is constituted of one unique α-SiW_9O_{34} unit, two crystallographically different cations (cerium for **1** and uranium for **2**) and one acetate ligand. The complete molecule is obtained by the application of an inversion center located between the two μ^3-oxo bridges. The external cation (Ce or U) is coordinated by two $[SiW_9O_{34}]^{10-}$ units via five oxygen atoms of the vacancies of the POMs. Its coordination sphere is completed by one μ^3-oxo bridge and one chelating acetate ligand positioned in an almost-equatorial fashion, compared to the axis of the two $[SiW_9O_{34}]$ units. In contrast, the internal metallic cation (Ce or U) is close to the inversion center of the molecular species and is coordinated by the two μ^3-oxo bridges and the two $[SiW_9O_{34}]$ units via six oxygen atoms (Figure 2a). Careful

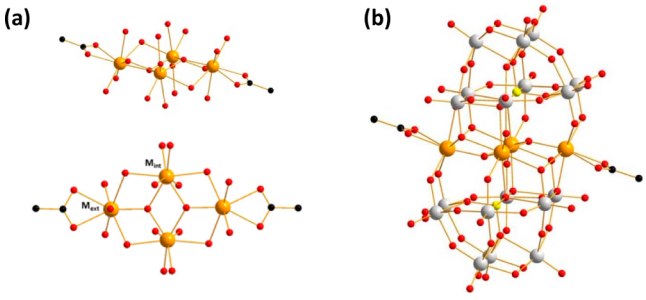

Figure 2. Ball and stick representation of the tetranuclear subunit-based compounds **1** and **2**: (a) top and side views of the tetranuclear cluster and (b) view of the sandwich architecture.

examination of the distances in both tetranuclear clusters (Table 2) reveals a small increase of several distances for the compound containing the uranium. These modifications are due to the slight increase in ionic radius when going from cerium(IV) (1.11 Å) to uranium(IV) (1.14 Å).[52] The equatorial distances between the oxygen atoms of the polyanion and the cation are roughly equal for the internal cation (2.237(5)−2.406(5) Å for **1**, compared with 2.254(12)−2.398(11) Å for **2**). The same observation is made with the external atoms (average 2.485 Å for **1** and 2.484 Å for **2**), but their M−(μ^3-O) distances are longer for **2** (2.144(11) Å) than for **1** (2.128(5) Å). This structural observation shows that the sandwich complex with cerium is more compact than that with uranium, causing the external cation to be slightly off-center from the compound. It is worth noting that a mirror plane is present in the molecular unit. This plane goes through the inversion center and the silicon atoms of the POMs. Furthermore, a C_2 axis going through the two inner cerium atoms is also present. Thus, the molecular unit in this system possesses a C_{2h} symmetry. In these compounds, it is interesting to notice the occurrence of Archimedean square antiprismatic units MO_8 involved in a tetranuclear subcluster, which differs from that existing in a fluorite-type structure, with a regular cubic environment for the metallic element. The electroneutrality of both compounds is ensured by the presence of mixture of alkali metals. In both structures, three Cs^+ and seven Na^+ cations surrounded by water molecules or terminal oxygen atoms of the $[SiW_9O_{34}]$ unit were crystallographically located.

In compound **3**, the three thorium cations have a coordination number of seven. This coordination sphere was confirmed by BVS calculation performed by considering a coordination number of seven or nine for the cation (Table S2).[50,51] From these values, a coordination number of seven fitted best with the tetravalent nature of the thorium. Compound **3** crystallizes in a $P6_3/m$ hexagonal space group. The asymmetric unit is composed of one thorium atom, one $\{W_3O_{13}\}$ group belonging to the SiW_9O_{34} unit, and an oxygen atom corresponding to a μ^2-hydroxo bridge. Another oxygen atom type adopts a μ^3-oxo bridging mode, with a 1/6 multiplicity located on a C_3-axis. The silicon atom is also located on this axis. Application of the C_3 symmetry axis going through the silicon atom and the oxygen atom of the μ^3-oxo bridge and application of a mirror plane going through the $\{Th_3O_4\}$ central core give the complete sandwich-type molecule. The mirror planes parallel and perpendicular to the principal axis in the molecular structures define an average D_{3h} symmetry for the compound (Figure 3b). In the molecular structure, each of the three cations share four oxygen atoms with the two $[SiW_9O_{34}]$ units with distances ranging from 2.400(4) Å to 2.406(4) Å. The distances observed for the μ^2-hydroxo ranges from 2.422(9) Å to 2.425(9) Å and those of the μ^3-oxo bridges are of 2.267(3) Å. Electroneutrality of compound **3** is ensured by a mixture of 10 Na^+ and 3 Rb^+ cations located in the lattice of the molecule. All cations are located around the polyanion architecture, interacting with some terminal oxygen atoms of the $[SiW_9O_{34}]$ subunits and surrounded by several water molecules. This type of trinuclear arrangement possessing a μ^3-oxo bridge is unique in the chemistry of thorium. A similar arrangement with a μ^3-oxo bridge has already been observed for the U^{4+} cation in a coordination polymer based on U^{4+}−trimesate coordination.[53] As far as we know, only one example of trinuclear thorium arrangement has been reported in the literature.[54] The structure of this thorium cluster differs largely from our compound because the three thorium cations are bridged by six μ^2-hydroxo atoms to form a trinuclear $[Th_3(OH)_6]^{6+}$ unit; however, no μ^3-oxo bridge is present. In this literature compound, each thorium atom is thus coordinated to four μ^2-hydroxo groups. Its coordination sphere is completed by

DOI: 10.1021/acs.inorgchem.5b00786
Inorg. Chem. XXXX, XXX, XXX−XXX

Table 2. Comparison of Bond Distances for Compounds 1 and 2

	Compound 1		Compound 2	
	Ce_{int}	Ce_{ext}	U_{int}	U_{ext}
M−(O_{POMax}) (Å)	2.548(5)−2.565(5)	2.269(6)−2.400(6)	2.574(11)−2.606(11)	2.312(12)−2.408(12)
M−(O_{POMeq}) (Å)	2.237(5)−2.406(5)	2.482(5)−2.488(5)	2.254(12)−2.398(11)	2.479(11)−2.490(11)
M−(μ^3-O) (Å)	2.220(5)−2.231(5)	2.128(5)	2.248(11)−2.252(11)	2.144(11)
M−(O_{Ac}) (Å)		2.461(5)−2.463(5)		2.482(12)−2.497(12)

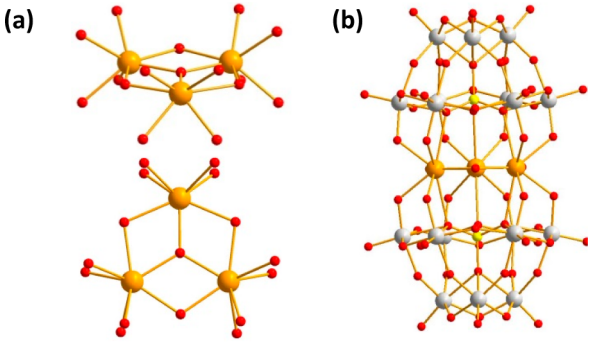

Figure 3. Ball-and-stick representation of the trimeric compound 3: (a) top and side views of the trimetallic cluster and (b) view of the sandwich architecture.

four nitrogen atoms belonging to a porphyrin molecule to give all three thorium atoms a square antiprism geometry.

In compound 4, the three hafnium centers possess a coordination number of six with a trigonal prismatic geometry. BVS calculations confirmed the +4 character of each hafnium cation in this geometry. Each hafnium atom is coordinated to four oxygen atoms belonging to the two polyoxometalates (from 2.076(8) Å to 2.118(8) Å) and two atoms belonging to the μ^2-OH bridges (from 2.041(8) Å to 2.112(8) Å). The compound crystallized in the triclinic $P\bar{1}$ space group. The inversion center is located outside the molecular unit and, the anionic part of the compound contains a chloride atom located on this inversion center with a multiplicity of 1/2. It is probably coming from the chloride hafnium salt used in the synthesis. The molecular unit possesses a C_3-axis going through the two Si atoms of the POMs. Three mirrors parallel and on mirror perpendicular to the main C_3-axis give the molecule a D_{3h} symmetry. Electroneutrality is ensured by three sodium and 8.5 Rb^+ cations surrounded by water molecules and oxygen atoms from the $[SiW_9O_{34}]$ unit.

The major difference between the two isostructural compounds 1 and 2 and compound 3 lies in the nuclearity of the polyoxo subcluster stabilized by the two SiW_9O_{34} moieties. From the four tetravalent cations used in these studies, the compound bearing thorium possesses the largest ionic radius (1.19 Å),[52] giving it a soft acid character, greatly favoring olation condensation processes, compared to U^{4+} and Ce^{4+}, which are harder acids and are more easily condensed by oxolation processes. From a general point of view, increasing the nuclearity of a cluster is easier when it is monitored by oxolation condensation reaction rather than olation reaction. This phenomenon could explain why, under the same synthetic conditions, the nuclearity of the thorium cluster is limited to three. This cluster has three hydroxo bridges and only one oxo bridge, whereas with uranium and cerium, the clusters are tetrameric and constructed around two oxo bridges. The molecular arrangement observed for compound 4 slightly differs from the other trinuclear cluster with thorium. Because of the smaller ionic radius of the hafnium cation (0.97 Å), its coordination number is generally limited to six, similar to that observed for most of the 3d or 4d transition metals (although some rare examples present higher coordination numbers).[55] This preferential coordination number limits the nuclearity of the cluster to a simple trinuclear cluster fragment, in agreement with the C_3 symmetry of the polyanion, without any μ^3-O bridge. This arrangement with three μ^2-OH bridges has already been observed with the zirconium cation (ionic radius = 0.98 Å).[29] In our species, the distances between the metallic cation and the oxygen atoms belonging to the two silicotungstic units and the oxygen atoms of the hydroxo bridges are in the same range (M−-O_{POM} = 2.04(2)−2.16(2) Å from ref 29 and 2.076(8)−2.118(8) Å for (4)) and M−OH-M = 2.06(2)−2.13(2) Å from ref 29 and 2.041(8)−2.112(8) Å for (4)), in agreement with the close ionic radii of both cations.

Thermal Behavior. Thermogravimetric (TG) analyses were performed on the compounds to determine the water content of the systems (Figure S4 in the Supporting Information). Calculations were carried out based on the observation of the first loss of weight (i.e., 200 °C for compound 1, 260 °C for compounds 2 and 4) and compared with the calculated values obtained from the RX studies. They indicated that the three compounds contain 40 (obs., 11.5%; calc., 8.4%), 24 (obs., 6.8%; calc., 6.6%), and 24 (obs., 6.9%; calc., 6.6%) hydration water molecules for the cerium, uranium, and hafnium clusters, respectively. From the structural point of view, all the water molecules could not be found from the XRD studies, because of the important disorder of the water molecules, which is a classical issue in polyoxometalate systems provoking differences between calculated and observed percentages. For the first two systems, a second weight decrease can be observed until 400 °C for 1 and 500 °C for 2. This step could correspond to the loss of the organic part (acetate ligand) coordinated to the cerium and the uranium. From the calculations, 3 acetate molecules (obs., 3.2%; calc., 1.97%) and 1.5 acetate molecules (obs., 1.24%; calc., 1.88%) are lost for compounds 1 and 2, respectively (two molecules being coordinated to the cluster). At higher temperature, a small increase in weight is observed for the uranium compound. It could correspond to the formation of uranium oxide (U_3O_8). Since compound 3 was not obtained pure, no TG measurement was performed.

Infrared Spectroscopy and Powder Diffraction. The infrared (IR) spectra of four compounds was collected and compared to the one of the SiW_9O_{34} precursors (Figure 4). Informations regarding the POM moiety can be obtained in the range of 1100−400 cm^{-1}. This domain corresponds to W−O and Si−O vibrations. The latter ones are generally overlapped with the W−O vibrations in the cases of silicotungstate compounds. From the spectra, it appears that the polyanion backbone is strongly modified, which is consistent with the coordination of heterometals on the POM vacancies. We mainly observed some variations at ∼15−25 cm^{-1} from the

DOI: 10.1021/acs.inorgchem.5b00786
Inorg. Chem. XXXX, XXX, XXX−XXX

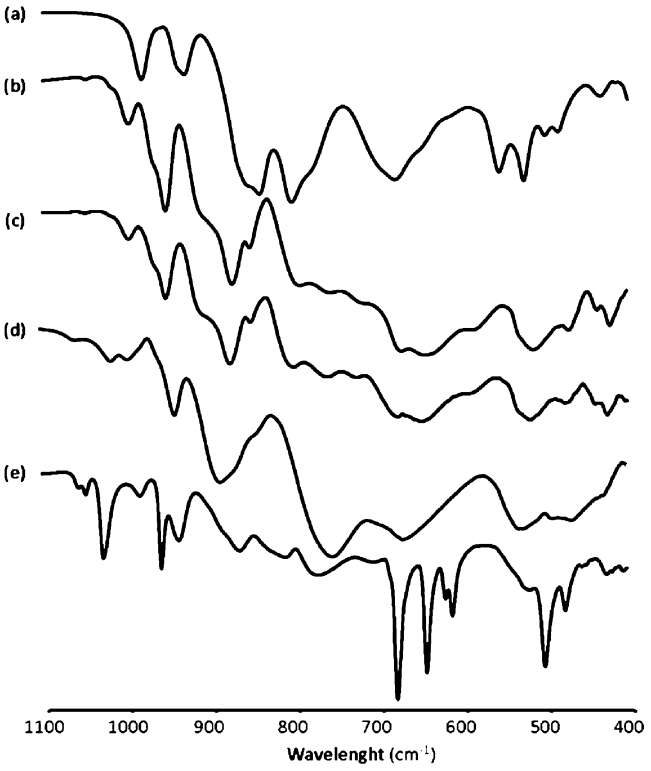

Figure 4. IR spectra in the polyoxometalate region of $\{SiW_9O_{34}\}$ (spectrum a), $\{Ce_4(\mu^3\text{-}O)_2(SiW_9O_{34})_2(OAc)_2\}$ (spectrum b), $\{U_4(\mu^3\text{-}O)_2(SiW_9O_{34})_2(OAc)_2\}$ (spectrum c), $\{Hf_3(\mu^2\text{-}OH)_3(SiW_9O_{34})_2\}$ (spectrum d), and $\{Th_3(\mu^3\text{-}O)(\mu^2\text{-}O)_3(SiW_9O_{34})_2\}$ (spectrum e).

W−Ob−W, W−Oc−W, and W−Od vibrations (see Table S1 in the Supporting Information). Spectra of compounds **1** and **2** are almost similar, and this confirms the same mode of coordination of the cerium and the uranium clusters to the SiW_9O_{34} polyanion. The spectrum of compound **4** shows slightly modified W−Ob−W, W−Oc−W, and W−Od vibrations, in comparison with compounds **1** and **2**. This difference must be assigned to the different coordination geometries (prismatic) of the hafnium atoms constituting the trinuclear cluster. The spectrum of the thorium-containing compound **3** appears different than the other ones, and important vibrations that did not belong to the sandwich compound are observed. They are, in a large part, due to impurities that are present in the crystallized preparation. This impurity was clearly identified by powder XRD analysis (see the powder patterns in Figure S2) and IR spectroscopy. It consists of a polymeric chain based on the coordination of acetates around the thorium cation. For instance, the comparison of the calculated XRD pattern of the $U^{IV}(CH_3COO)_4$ chain with our impurities shows close diffraction Bragg peaks with a slight shift in the lower θ region, in agreement with the greater ionic radius of the thorium over the uranium.[56] The presence of these acetate ligands is also visible in the IR spectrum in the region of 1400−1600 cm^{-1} (not shown) and in the POM region below 1100 cm^{-1}, where several vibrations belonging to the organic component are visible (Figure 4). Finally, comparison of simulated powder patterns obtained from the structural resolution with the experimental ones show that compounds **1**, **2**, and **4** are obtained as a pure crystalline phase (Figure 5).

Ultraviolet−Visible (UV-vis) Spectroscopy. It is well-known from the literature that U^{4+}-containing systems exhibit characteristic transitions in the visible region, but very few data exist regarding its association with polyoxometalates.[17,46] The spectrum of the $\{U^{IV}_4(SiW_9O_{34})_2\}$ system was recorded between 400 and 900 nm both in solution and in solid state (Figure S3 in the Supporting Information). The spectra present very broad absorbance but some transitions are still observable. They concern two U^{4+}−W^{6+} transitions: $^3H_4$ to $^3P_2$ at 431 nm, $^3H_4$ to $^3P_1$ at 552 nm, and two f-f transitions of U^{4+}: $^3H_4$ to $^3P_0$ at 644 nm and $^3H_4$ to $^1D_2$ at 665 nm. All these transitions are characteristic of a U^{4+}-containing species. In the solid state, the transitions are much broader and almost disappear, probably because of the charge-transfer interactions occurring between the U^{4+} and the W^{6+} of the polyanion.[17]

^{183}W and ^{29}Si NMR Studies. Solution stabilities studies of compounds **1** and **4** were performed by ^{29}Si and ^{183}W NMR experiments. The ^{29}Si spectra were recorded using a solution that contained a concentration of compound of ∼25 mmol L^{-1}. They both show only one single moderately sharp signal, in agreement with 2 equiv of $[SiW_9O_{34}]$ unit in each compound, respectively located at −84 ppm and −85 ppm for molecule **1** and **4** with a line width ($\Delta\nu_{1/2}$) of 10 Hz (see Figure S5 in the Supporting Information). ^{183}W NMR spectra of the two systems and the chemical shift with the related intensities are respectively shown in Figure 6 and Table 3. The spectrum of $\{Ce_4(\mu^3\text{-}O)_2(SiW_9O_{34})_2(CH_3COO)_2\}$ exhibits a five-line setup with resonances going from −147.9 ppm to −180.2 ppm, with a relative intensity of 1:2:2:2:2. The chemical shifts are located in the usual range for tungsten atoms in an octahedral oxygen environment. The molecular compound possess a plane of symmetry going through the two external cerium atoms and a C_2 axis going through the two inner cerium atoms giving a global C_{2h} symmetry for the compound. The combination of ^{29}Si and ^{183}W NMR signals is consistent with this C_{2h} symmetry. The resonances located at −147.9 ppm and −174.4 ppm appear to be slightly broadened ($\Delta\nu_{1/2}$ = 7.9−9.4 Hz) and could correspond to the three tungsten atoms of the $[SiW_9O_{34}]$ cap, the three others sharper signals ($\Delta\nu_{1/2}$ = 5.3−7.5 Hz) being related to the six tungsten atoms of the polyanion belt. Compound $\{Hf_3(\mu^2\text{-}OH)_3(SiW_9O_{34})_2\}$ presents a two-line spectrum with a relative intensity of 2:1, respectively located at −145 and −175 ppm, in the usual range for polyoxometalates. This observation combined with the ^{29}Si spectrum is reliable, with an average D_{3h} symmetry of the molecular unit of the compound in solution. The sharp signal ($\Delta\nu_{1/2}$ = 5.3 Hz) at −175 ppm is related to the three tungsten atoms of the cap and the very broad signal centered at −145 ppm is attributed to the six atoms of the belt. This signal appears to be affected by moderately slow dynamic proton hopping occurring between protons of solvent (H_2O−D_2O) and oxygen atoms belonging to the μ^2-OH bridges of the $\{Hf_3O_3\}$ moieties. BVS calculation of O71 (1.43) shows that it is slightly different than O69 (1.24) and O70 (1.21). Furthermore, the distances are shorter for Hf−O71 bonds (average 2.045 Å) than Hf−O69 bonds (2.10 Å) or Hf−O70 bonds (2.109 Å). We stated in the crystallographic study that the three bridges of the trinuclear hafnium belt are protonated; however, based on the distances and BVS, it remains possible that one of the three oxygen bridges (O71) could be partially deprotonated, allowing this proton hopping and causing the broadening of the signal centered at −145 ppm. Nevertheless, these multiplicities observations confirm the stability of both compounds in solution, at least over the measurement period (4 days) needed to obtain the spectra.

DOI: 10.1021/acs.inorgchem.5b00786
Inorg. Chem. XXXX, XXX, XXX−XXX

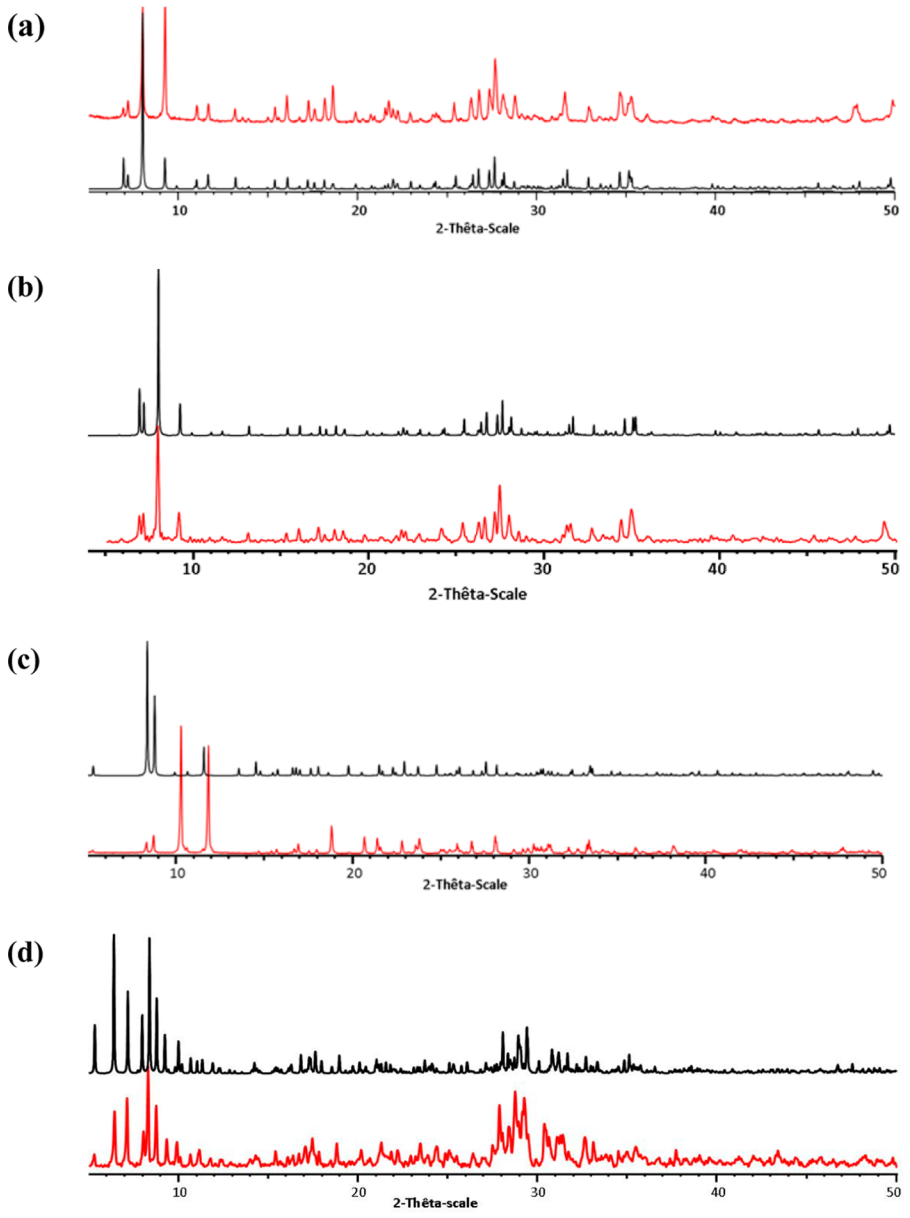

Figure 5. Calculated (black line) and experimental (red line) powder X-ray diffraction (XRD) patterns of $[Ce^{IV}_4(\mu^3\text{-}O)_2(SiW_9O_{34})_2(CH_3COO)_2]\cdot 40H_2O$ (spectrum a), $[U^{IV}_4(\mu^3\text{-}O)_2(SiW_9O_{34})_2(CH_3COO)_2]\cdot 24H_2O$ (spectrum b), $[Th^{IV}_3(\mu^3\text{-}O)(\mu^3\text{-}O)_3(SiW_9O_{34})_2]$ (spectrum c), and $[Hf_3(\mu^2\text{-}OH)_3(SiW_9O_{34})_2]\cdot 24H_2O$ (spectrum d).

Magnetism. To ascertain the formal valence of the uranium ions, we investigated the magnetic properties of compound **2** as a function of temperature. The temperature variation of the magnetic susceptibility and the magnetization curve at 1.8 K is shown in Figure S6 in the Supporting Information. The magnetic susceptibility ($\chi(T)$) increases continuously between room temperature and 1.8 K, with a slight upturn below 15 K. Consistently, the χT product decreases from 3.74 K emu mol^{-1} at 300 K (0.94 K emu/U mol) to 0.15 K emu mol^{-1} at 1.8 K (0.04 K emu/U mol). The constant decrease of the χT vs T curve indicates the predominance of temperature-dependent effects. On this basis, we have tentatively fit the temperature variation of the magnetic susceptibility by using the relation $\chi = C/(T + A) + B$. The first term holds for localized electron systems within the frame of crystal field approach, which is usually the starting point for analyzing the properties of actinide systems.[57] The parameter B is often introduced to take into account possible electron delocalization (and Pauli paramagnetism), yet it can phenomenologically be used to account for other temperature-independent effects, including van Vleck paramagnetism.[57,58] The value of the Curie constant (C) is dependent on the effective moment: $\mu_{eff}^2 = 8C$.

As shown in Figure S6, a nice fit of our experimental data was obtained above 15 K, with refined values of C = 2.50(1) K emu mol^{-1}, A = 71.7(3) K, and B = 0.00595(3) emu mol^{-1}. The parameter B is quite large. In the present case, we do not expect much delocalization, since the shortest inter-ion distance (U_{int}–U_{int} = 3.68 Å) is higher than the critical distance reported for the occurrence of inter-ion interaction (3.4–3.6 Å).[57] Hence, B most likely reflects the occurrence of coupling between the ground state and excited states leading to van Vleck paramagnetism. It is worth noting that any error in the diamagnetic correction can also contribute to the value of B. From the C value for tetrameric units, we can deduce the

DOI: 10.1021/acs.inorgchem.5b00786
Inorg. Chem. XXXX, XXX, XXX–XXX

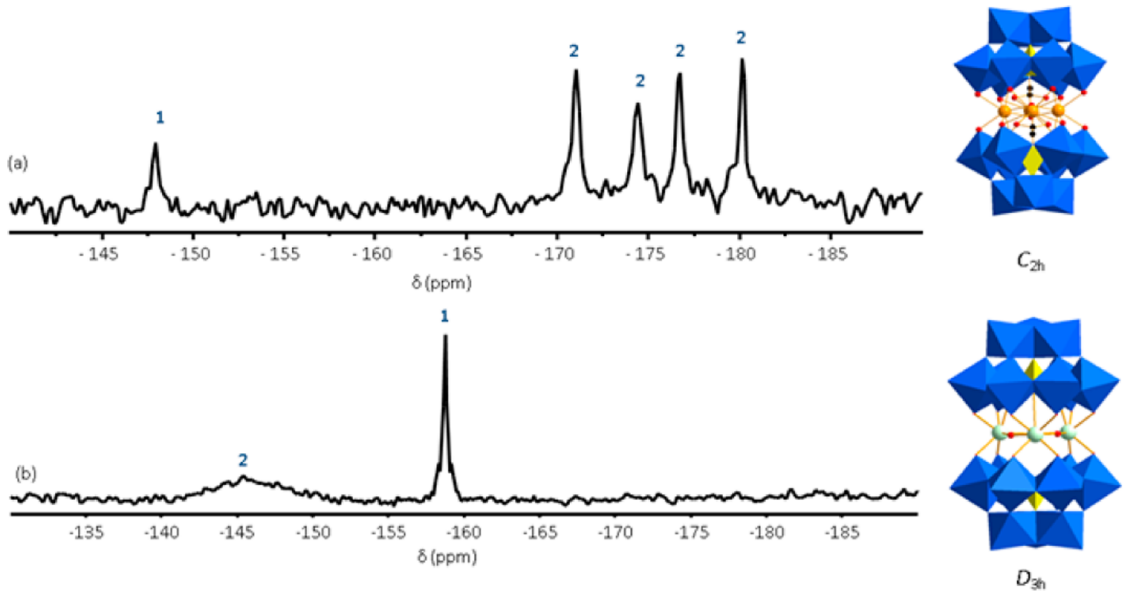

Figure 6. ^{183}W NMR spectra of $\{Ce_4(\mu^3\text{-}O)_2(SiW_9O_{34})_2(CH_3COO)_2\}$ (spectrum a) and $\{Hf_3(\mu^2\text{-}OH)_3(SiW_9O_{34})_2\}$ (spectrum b).

Table 3. ^{183}W Chemical Shifts for Compounds 1 and 4

	δ (ppm)/Relative Intensity/$\Delta\nu_{1/2}$ (Hz)	
compound	belt	cap
$\{Ce_4(\mu^3\text{-}O)_2(SiW_9O_{34})_2(CH_3COO)_2\}$, **1**	−171/2/6.5	−147.9/1/7.9
	−176.7/2/7.5	−174.4/2/9.4
	−180.2/2/5.3	
$\{Hf_3(\mu^2\text{-}OH)_3(SiW_9O_{34})_2\}$, **4**	−145/2/not measured	−175/1/5.3

effective moment μ_{eff} = 3.5 μ_B per U^{IV} atoms. The μ_{eff} value at room temperature is consistent with that found in the literature for U^{4+} ions (2.5−3.5 μ_B /U),[46,59−62] especially in polyoxometalates.[46,63,64] Below 15 K, a steeper increase of the magnetic susceptibility is observed. Such changes in the magnetic behavior can stem either from ion−ion interactions or changing populations of low-lying crystal field states. The magnetization versus field curve at low temperature, $M(H)$, indicates a small magnetic moment for the $\{U^{IV}_4(SiW_9O_{34})_2\}$ compound (**2**). This paramagnetic behavior agrees with a coupling of the nonmagnetic ($^3H_4$, m_J = 0) ground state with low-lying excited states.[59−61,65] The overall magnetic behavior is consistent with what was reported in the literature for U^{4+} compounds within the localized electron model.[34,61,62,65−67]

4. CONCLUSION

A simple synthetic strategy was adopted and efficiently applied to obtain four new compounds based on the trivacant $[SiW_9O_{34}]^{10-}$ building block. Association of this polyanion with Ce^{4+} or U^{4+} give us the isostructural moieties $[M^{IV}_4(\mu^3\text{-}O)_2(SiW_9O_{34})_2(CH_3COO)_2]^{10-}$ (**1** and **2**) containing a tetranuclear core. Surprisingly, the use of Th^{4+} leads only to the formation of a molecule $[Th_3(\mu^3\text{-}O)(\mu^2\text{-}OH)_3(SiW_9O_{34})_2]^{13-}$ (**3**) constructed around the trinuclear cationic core. Compound **4**, which involved the hafnium cation ($[Hf_3(\mu^2\text{-}OH)_3(SiW_9O_{34})_2]^{11-}$), is also arranged in a trinuclear core but with the absence of the μ^3-O bridge, relevant to the geometry of this type of cation. In the four compounds, the inorganic moieties play an interesting role in stabilizing these polymetallic tetravalent species to a discrete nanometric molecular level. The main structural difference on the topologies of the cluster is mainly due to the ionic radius of the cation, the biggest one (i.e., the thorium) being the most difficult to grown in nuclearity. As far as we know, these compounds are the first examples of polynuclear tetravalent (4f or 5f) clusters stabilized by polyoxometalate ligands that have been unambiguously characterized by X-ray diffraction. In addition, the solution studies carried out by 1D ^{29}Si and ^{183}W NMR measurements attested of the stability in solution of the tetrameric cerium and trimeric hafnium clusters associations. The magnetic behavior of the $\{U^{IV}_4(SiW_9O_{34})_2\}$ compound (**2**) is fully consistent with the presence of U^{IV} ions. These results open the pathway for further works regarding the use of POMs to bind and stabilize tetravalent cations clusters. We are currently working on pH and stoichiometric modulation to see their impact on the sizes and topologies of the obtained clusters.

■ ASSOCIATED CONTENT

Supporting Information

The Supporting Information is available free of charge on the ACS Publications website at DOI: 10.1021/acs.inorgchem.5b00786.

Synthesis details for UCl_4; comparison of $\{SiW_9O_{34}\}$ main vibrations of compounds **1**−**4** (Table S1); BVS data for compounds **1**−**4** (Table S2); SEM images of compounds **1**−**4** (Figure S1); calculated XRD spectra for $U^{IV}(CH_3COO)_4$ and experimental spectra for $Th^{IV}_3(\mu^3\text{-}O)(\mu^3\text{-}O)_3(SiW_9O_{34})_2$ (Figure S2); UV-vis spectra of $[U^{IV}_4(\mu^3\text{-}O)_2(SiW_9O_{34})_2(CH_3COO)_2]\cdot 24H_2O$ (Figure S3); TGA curves of $[Ce_4(\mu^3\text{-}O)_2(SiW_9O_{34})_2(CH_3COO)_2]\cdot 40H_2O$, $[U_4(\mu^3\text{-}$

DOI: 10.1021/acs.inorgchem.5b00786
Inorg. Chem. XXXX, XXX, XXX−XXX

$O)_2(SiW_9O_{34})_2(CH_3COO)_2]\cdot 24H_2O$, and $[Hf_3(\mu^2\text{-}OH)_3(SiW_9O_{34})_2]\cdot 24H_2O$ (Figure S4); ^{29}Si NMR spectra of $Ce_4(\mu^3\text{-}O)_2(SiW_9O_{34})_2(CH_3COO)_2$ and $Hf_3(\mu^2\text{-}OH)_3(SiW_9O_{34})_2$ (Figure S5); magnetization and magnetic susceptibility data for compound **2** (Figure S6); and EDX measurements for compounds **2** and **3** (Figure S7) (PDF)

Crystallographic data for $C_4H_6Ce_4Cs_{1.5}Na_{8.5}O_{97.5}Si_2W_{18}$ (**1**) (CIF)

Crystallographic data for $C_4H_6U_4Cs_3Na_7O_{97.7}Si_2W_{18}$ (**2**) (CIF)

Crystallographic data for $Na_{12}RbO_{98}Si_2Th_3W_{18}$ (**3**) (CIF)

Crystallographic data for $Na_3Rb_{8.5}O_{95.25}Cl_{0.5}Si_2Hf_3W_{18}$ (**4**) (CIF)

AUTHOR INFORMATION

Corresponding Author

*Tel.: (33) 3 20 434 973. Fax: (33) 3 20 43 48 95. E-mail: sylvain.duval@univ-lille1.fr.

Notes

The authors declare no competing financial interest.

ACKNOWLEDGMENTS

The authors would like to thank Mrs. Nora Djelal, Laurence Burylo, and Mr. Philippe Devaux for their technical assistances with the SEM images, TG measurements, and powder XRD (UCCS). The "Fonds Européen de Développement Régional (FEDER)", "CNRS", "Région Nord Pas-de-Calais", and "Ministère de l'Education Nationale de l'Enseignement Supérieur et de la Recherche" are acknowledged for funding of X-ray diffractometers. The present work is part of the research activity supported by the Labex NIE (Nanostructires in Interaction with their Environment, http://www.labex-nie.com/).

REFERENCES

(1) Pope, M. T.; Kortz, U. *Encyclopedia of Inorganic and Bioinorganic Chemistry*; John Wiley & Sons, Ltd.: New York, 2012.

(2) Pope, M. T. *Heteropoly and Isopoly Oxometalates*; Springer: Berlin, 1983.

(3) Pope, M. T.; Müller, A. *Angew. Chem., Int. Ed. Engl.* **1991**, *30*, 34–48.

(4) Pope, M. T., Müller, A., Eds. *Polyoxometallates: From Platonic Solids to Anti-Retroviral Activity*; Kluwer Academic Publishers: Dordrecht, The Netherlands, 1994.

(5) Dolbecq, A.; Dumas, E.; Mayer, C. R.; Mialane, P. *Chem. Rev.* **2010**, *110*, 6009–6048.

(6) Long, D. L.; Tsunashima, R.; Cronin, L. *Angew. Chem., Int. Ed.* **2010**, *49*, 1736–1758.

(7) Hill, C. L. *Chem. Rev.* **1998**, *98*, 1–390.

(8) Proust, A.; Matt, B.; Villanneau, R.; Guillemot, G.; Gouzerh, P.; Izzet, G. *Chem. Soc. Rev.* **2012**, *41*, 7605–7622.

(9) Molina, P. I.; Miras, H. N.; Long, D. L.; Cronin, L. *Dalton Trans.* **2014**, *43*, 5190–5199.

(10) Leclerc-Laronze, N.; Marrot, J.; Haouas, M.; Taulelle, F.; Cadot, E. *Eur. J. Inorg. Chem.* **2008**, *2008*, 4920–4926.

(11) Bassil, B. S.; Dickman, M. H.; Kortz, U. *Inorg. Chem.* **2006**, *45*, 2394–2396.

(12) Stracke, J. J.; Finke, R. G. *J. Am. Chem. Soc.* **2011**, *133*, 14872–14875.

(13) Assran, A. S.; Mal, S. S.; Izarova, N. V.; Banerjee, A.; Suchopar, A.; Sadakane, M.; Kortz, U. *Dalton Trans.* **2011**, *40*, 2920–2925.

(14) Iball, J.; Low, J. N.; Weakley, T. J. R. *J. Chem. Soc., Dalton Trans.* **1974**, 2021–2024.

(15) Iijima, J.; Naruke, H. *J. Mol. Struct.* **2013**, *1040*, 33–38.

(16) Ostuni, A.; Bachman, R. E.; Pope, M. T. *J. Cluster Sci.* **2003**, *14*, 431–446.

(17) Rusu, M.; Marcu, G.; Rusu, D.; Rosu, C.; Tomsa, A. R. *J. Radioanal. Nucl. Chem.* **1999**, *242*, 467–472.

(18) Sokolova, M. N.; Fedosseev, A. M.; Andreev, G. B.; Budantseva, N. A.; Yusov, A. B.; Moisy, P. *Inorg. Chem.* **2009**, *48*, 9185–9190.

(19) Tourne, C. M.; Tourne, G. F.; Brianso, M. C. *Acta Crystallogr., Sect. B: Struct. Crystallogr. Cryst. Chem.* **1980**, *36*, 2012–2018.

(20) Fang, X.; Koegerler, P. *Angew. Chem., Int. Ed.* **2008**, *47*, 8123–8126.

(21) Reinoso, S.; Galan-Mascaros, J. R.; Lezama, L. *Inorg. Chem.* **2011**, *50*, 9587–9593.

(22) Bassil, B. S.; Mal, S. S.; Dickman, M. H.; Kortz, U.; Oelrich, H.; Walder, L. *J. Am. Chem. Soc.* **2008**, *130*, 6696–6697.

(23) Hou, Y.; Fang, X.; Hill, C. L. *Chem.—Eur. J.* **2007**, *13*, 9442–9447.

(24) Kato, C. N.; Shinohara, A.; Hayashi, K.; Nomiya, K. *Inorg. Chem.* **2006**, *45*, 8108–8119.

(25) Kikukawa, Y.; Yamaguchi, S.; Tsuchida, K.; Nakagawa, Y.; Uehara, K.; Yamaguchi, K.; Mizuno, N. *J. Am. Chem. Soc.* **2008**, *130*, 5472–5478.

(26) Nomiya, K.; Saku, Y.; Yamada, S.; Takahashi, W.; Sekiya, H.; Shinohara, A.; Ishimaru, M.; Sakai, Y. *Dalton Trans.* **2009**, 5504–5511.

(27) Sokolov, M. N.; Chubarova, E. V.; Peresypkina, E. V.; Virovets, A. V.; Fedin, V. P. *Russ. Chem. Bull.* **2007**, *56*, 220–224.

(28) Bion, L.; Moisy, P.; Madic, C. *Radiochim. Acta* **1995**, *69*, 251–257.

(29) Finke, R. G.; Rapko, B.; Weakley, T. J. R. *Inorg. Chem.* **1989**, *28*, 1573–1579.

(30) Al-Kadamany, G.; Mal, S. S.; Milev, B.; Donoeva, B. G.; Maksimovskaya, R. I.; Kholdeeva, O. A.; Kortz, U. *Chem.—Eur. J.* **2010**, *16*, 11797–11800.

(31) Shiryaev, A. A.; Shilov, V. P.; Fedoseev, A. M.; Volkov, V. V. *Radiochemistry* **2014**, *56*, 489–492.

(32) Knope, K. E.; Vasiliu, M.; Dixon, D. A.; Soderholm, L. *Inorg. Chem.* **2012**, *51*, 4239–4249.

(33) Malaestean, I. L.; Ellern, A.; Baca, S.; Kogerler, P. *Chem. Commun.* **2012**, *48*, 1499–1501.

(34) Falaise, C.; Volkringer, C.; Vigier, J. F.; Beaurain, A.; Roussel, P.; Rabu, P.; Loiseau, T. *J. Am. Chem. Soc.* **2013**, *135*, 15678–15681.

(35) Knope, K. E.; Soderholm, L. *Chem. Rev.* **2013**, *113*, 944–994.

(36) Nyman, M.; Burns, P. C. *Chem. Soc. Rev.* **2012**, *41*, 7354–7367.

(37) Tézé, A.; Hervé, G. *Inorganic Syntheses*, Vol. *27*; John Wiley and Sons: Hoboken, NJ, 1990; p 85.

(38) Navaza, A.; Charpin, P.; Vigner, D.; Heger, G. *Acta Crystallogr., Sect. C: Cryst. Struct. Commun.* **1991**, *47*, 1842–1845.

(39) *SAINT Plus, Version 7.53a*; Bruker Analytical X-ray Systems: Madison, WI, 2008.

(40) Sheldrick, G. M. *SADABS, Bruker–Siemens Area Detector Absorption and Other Correction, Version 2008/1*; Bruker: Madison, WI, 2008.

(41) Sheldrick, G. M. *Acta Crystallogr., Sect. A: Found. Crystallogr.* **2008**, *64*, 112–122.

(42) Pascal, P. *Annal. Chim. Phys.* **1910**, *19*, 5–70.

(43) Bain, G. A.; Berry, J. F. *J. Chem. Educ.* **2008**, *85*, 532.

(44) Knope, K. E.; Wilson, R. E.; Vasiliu, M.; Dixon, D. A.; Soderholm, L. *Inorg. Chem.* **2011**, *50*, 9696–9704.

(45) Shilov, V. P.; Yusov, A. B.; Peretrukhin, V. F.; Delegard, C. H.; Gogolev, A. V.; Fedosseev, A. M.; Kazansky, L. P. *J. Alloys Compd.* **2007**, *444–445*, 333–338.

(46) Bion, L.; Moisy, P.; Vaufrey, F.; Meot-Reymond, S.; Simoni, E.; Madic, C. *Radiochim. Acta* **1997**, *78*, 73–82.

(47) Trzebiatowska, J. *J. Chem. Phys.* **1963**, *60*, 843.

(48) Hanuza, J.; Trzebiatowska, B. *Acta Phys. Pol., A* **1974**, *A45*, 885.

(49) Kiener, C.; Folcher, G.; Rigny, P.; Virlet, J. *Can. J. Chem.* **1976**, *54*, 303.

(50) Brese, N. E.; O'Keeffe, M. *Acta Crystallogr., Sect. B: Struct. Sci.* **1991**, *47*, 192–197.

(51) Roulhac, P. L.; Palenik, G. J. *Inorg. Chem.* **2003**, *42*, 118–121.

DOI: 10.1021/acs.inorgchem.5b00786
Inorg. Chem. XXXX, XXX, XXX–XXX

(52) Shannon, R. D. *Acta Crystallogr., Sect. A: Cryst. Phys., Diffr., Theor. Gen. Crystallogr.* **1976**, *32*, 751−767.
(53) Volkringer, C.; Mihalcea, I.; Vigier, J. F.; Beaurain, A.; Visseaux, M.; Loiseau, T. *Inorg. Chem.* **2011**, *50*, 11865−11867.
(54) Kadish, K. M.; Liu, Y. H.; Anderson, J. E.; Charpin, P.; Chevrier, G.; Lance, M.; Nierlich, M.; Vigner, D.; Dormond, A.; Belkalem, B.; Guilard, R. *J. Am. Chem. Soc.* **1988**, *110*, 6455−6462.
(55) Hagfeldt, C.; Kessler, V.; Persson, I. *Dalton Trans.* **2004**, 2142−2151.
(56) Jelenic, I.; Grdenic, D.; Bezjak, A. *Acta Crystallogr.* **1964**, *17*, 758.
(57) Lam, D. J.; Aldred, A. T. Magnetic properties of actinide compounds. In *The Actinides: Electronic Structure and Related Properties*; Freeman, A. J., Darby, J. B., Jr., Eds.; Academic Press: New York, 1974; Vol. *1*.
(58) Erdös, P.; Robinson, J. M. *The Physics of Actinide Compounds*; Plenum Press: New York, London, 1983.
(59) Nocton, G.; Pécaut, J.; Mazzanti, M. *Angew. Chem., Int. Ed.* **2008**, *47*, 3040−3042.
(60) Castro-Rodriguez, I.; Meyer, K. *Chem. Commun.* **2006**, 1353−1368.
(61) Newell, B. S.; Schwaab, T. C.; Shores, M. P. *Inorg. Chem.* **2011**, *50*, 12108−12115.
(62) Gamp, E.; Edelstein, N.; Malek, C. K.; Hubert, S.; Genet, M. *J. Chem. Phys.* **1983**, *79*, 2023−2026.
(63) Marcu, G.; Rusu, M. *Rev. Roum. Chim.* **1977**, *22*, 227.
(64) Marcu, G.; Rusu, M. *Rev. Roum. Chim.* **1977**, *22*, 849.
(65) Santini, P.; Carretta, S.; Amoretti, G.; Caciuffo, R.; Magnani, N.; Lander, G. H. *Rev. Mod. Phys.* **2009**, *81*, 807−863.
(66) Meskaldji, S.; Zaiter, A.; Belkhiri, L.; Boucekkine, A. *Theor. Chem. Acc.* **2012**, *131*, 1−10.
(67) Wen, X.-D.; Martin, R. L.; Henderson, T. M.; Scuseria, G. E. *Chem. Rev.* **2013**, *113*, 1063−1096.

DOI: 10.1021/acs.inorgchem.5b00786
Inorg. Chem. XXXX, XXX, XXX−XXX